Biochimica et Biophysica Acta 1838 (2014) 3069–3077

Contents lists available at ScienceDirect

Biochimica et Biophysica Acta

journal homepage: www.elsevier.com/locate/bbamem

A detailed analysis of partial molecular volumes in DPPC/cholesterol binary bilayers

Tsubasa Miyoshi [a,*], Max Lönnfors [b], J. Peter Slotte [b], Satoru Kato [a]

[a] Department of Physics, Graduate school of Science and Technology, Kwansei Gakuin University, 2-1 Gakuen, Sanda, Hyogo 669-1337, Japan
[b] Biochemistry, Department of Bioscience, Åbo Akademi University, Tykistökatu 6A, 20520 Turku, Finland

ARTICLE INFO

Article history:
Received 22 January 2014
Received in revised form 27 June 2014
Accepted 2 July 2014
Available online 21 August 2014

Keywords:
DPPC/cholesterol binary bilayer
Buoyant density measurement
Fluorescence decay
Liquid-ordered phase
Partial molecular volume
L_d/L_o phase coexistence

ABSTRACT

We examined the volumetric behavior of the dipalmitoylphosphatidylcholine (DPPC)/cholesterol binary bilayer system with high accuracy and more cholesterol concentrations to reveal the detailed molecular states in the liquid-disordered (L_d) phase, the liquid-ordered (L_o) phase and the gel phase. We measured the average specific volume of the binary bilayer at several temperatures by the neutral flotation method and calculated the average volume per molecule to estimate the partial molecular volumes of DPPC and cholesterol in each phase. As a result, we found that the region with intermediate cholesterol concentrations showed a more complicated behavior than expected from simple coexistence of L_d and L_o domains. We also measured fluorescence decay of *trans*-parinaric acid (tPA) added into the binary bilayer with more cholesterol concentrations to get further insight into the cholesterol-induced formation of the L_o phase. On the basis of these results we discuss the molecular interaction between DPPC and cholesterol molecule in the L_o phase and the manner of L_d/L_o phase coexistence.

1. Introduction

Cholesterol, one of the major components in biological membranes, is known to be a modulator of their physicochemical properties, and its membrane effects have been intensively studied using various experimental techniques such as differential scanning calorimetry [1–3], X-ray diffraction [4–8], nuclear magnetic resonance [9–12], fluorescence spectroscopy [13–16] and computer simulations [17–21]. Since the recognition of the existence of cholesterol-containing functional microdomains called 'lipid rafts' [22–24], lipid researchers have focused on clarifying the role of cholesterol in the raft formation using binary or ternary lipid systems [25–27]. In these artificial lipid bilayer systems, addition of cholesterol induces formation of the liquid-ordered (L_o) phase, which is thought to represent the physicochemical state of the lipid raft [28–30].

It has been reported that the L_o phase has intermediate properties between the liquid-disordered (L_d) phase and the gel phase [31]. Phase diagrams of phospholipid/sterol binary systems, which give fundamental information on the effect of cholesterol on the properties of the L_o phase, have been proposed by several researchers [26,32–35]. However, the detailed mechanism of the cholesterol-induced L_o phase formation in the molecular level is still unclear.

Simple volumetric measurements are useful because they are able to give quantitative information on the volume of each molecule in a binary lipid bilayer. Greenwood et al. [36] examined the effect of cholesterol on the molecular packing in phospholipid/cholesterol mixed bilayers by the neutral flotation method. They estimated the partial molecular volumes of phospholipid and cholesterol in the L_d and L_o phases on the basis of the dependence of the average molecular volume on cholesterol mole fraction. However, perhaps due to not measuring enough concentrations and temperatures, they did not report an L_d/L_o coexistence region, which has been reported to exist [26,32–35].

In this study, we re-examined the volumetric behavior of dipalmitoylphosphatidylcholine (DPPC)/cholesterol binary membranes with more cholesterol concentrations and temperatures and with similar accuracies of the measured density, the cholesterol concentration, and the temperature to those in the previous work by Greenwood et al. [36]. As a result, some regions were clearly discernible in the average molecular volume vs. cholesterol mole fraction plot, especially at temperatures above the main transition temperature of the pure DPPC bilayer. The partial molecular volumes of DPPC and cholesterol were obtained and found to be in agreement with those obtained for fluid phases by Greenwood et al. [36], but in disagreement with older gel phase data [37] that were also compiled [36]. In addition, the dependence of the average molecular volume on cholesterol mole fraction deviated from linearity expected from simple coexistence of the L_d and L_o domains, giving a new insight into coexistence properties.

Abbreviations: DPPC, 1,2-dipalmitoyl-*sn*-glycero-3-phosphocholine; L_d, liquid-disordered; L_o, liquid-ordered; D_2O, deuterium oxide; tPA, *trans*-parinaric acid

* Corresponding author. Tel.: +81 79 565 9730.
E-mail address: t.miyoshi@kwansei.ac.jp (T. Miyoshi).

http://dx.doi.org/10.1016/j.bbamem.2014.07.004
0005-2736/

2. Materials and methods

2.1. Materials

1,2-dipalmitoyl-*sn*-glycero-3-phosphocholine (DPPC) and cholesterol were purchased from Avanti Polar Lipids (Alabaster, AL) and used without further purification. Deuterium oxide (D_2O) and *trans*-parinaric acid (tPA) were obtained from Cambridge Isotope Laboratories (Andover, MA) and Cayman Chemical (Ann Arbor, MI), respectively.

2.2. Buoyant density measurement

The specific volume of the DPPC/cholesterol binary bilayer $\overline{v}(x_c)$ was determined according to the neutral flotation method described by Greenwood et al. [36], where x_c is the cholesterol mole fraction. Briefly, DPPC and cholesterol were separately dissolved in chloroform/methanol (4 : 1, v/v) and mixed at an appropriate mole ratio. The obtained solution was dried at 60 °C under nitrogen flow and in vacuum, and the resulting lipid film was dissolved into an H_2O/D_2O solvent, the density of which was adjusted to be as near as possible to that of the bilayer. After centrifugation (19, 800$g \times 10 - 20$ min) in a temperature-controlled centrifuge (Kubota, Model 5922), an aliquot of an H_2O/D_2O solvent with either higher or lower density than that of the solvent in the centrifugation tube was added according to whether the bilayers sedimented or floated. This procedure was repeated until the change in density by the addition of the solvent became less than 5×10^{-4}g/cm^3. As the bilayers were distributed as a fairly narrow band after the final centrifugation, the density difference between vesicles must be smaller than 5×10^{-4}g/cm^3. We repeated the measurement at least three times by using the data obtained in the last measurement as an initial density in the next measurement to eliminate the error caused by the difference in solvent density between inside and outside of the multi-lamellar vesicle.

In order to obtain the data with high accuracy, we added more than 10μL of the solvent for the density adjustment and used the D_2O solution as fresh as possible to prevent contamination of H_2O. Moreover, we checked the temperature of the sample solution after centrifugation and adopted the data for the density analysis only when the measured temperature was within ±0.5 °C of the desired temperature.

Fig. 1 shows how to estimate the partial molecular volume of each molecule in the binary system. The procedure of the analysis is based on that described by Greenwood et al. [36]. We calculated the average volume per molecule $\overline{V}(x_c)$ from the obtained specific volume of the binary bilayer $\overline{v}(x_c)$ by:

$$\overline{V}(x_c) = \frac{\overline{v}(x_c)}{N_A}\{(1-x_c)M_L + x_c M_c\}, \tag{1}$$

where N_A, M_L and M_c are Avogadro's number, the molecular weight of DPPC and the molecular weight of cholesterol, respectively (Fig. 1B). In order to make the deviation from linearity clearly visible, we subtracted a straight line from $\overline{V}(x_c)$:

$$\overline{V}^*(x_c) = \overline{V}(x_c) - Cx_c, \tag{2}$$

where C is the gradient of the straight line fitted to the data at lower x_c region (Fig. 1C). Assuming that the partial molecular volumes of DPPC (V_{DPPC}) and cholesterol (V_{chol}) are constant in a phase, $\overline{V}^*(x_c)$ gives a straight line as

$$\begin{aligned}\overline{V}^*(x_c) &= (1-x_c)V_{DPPC} + x_c V_{chol} - Cx_c \\ &= -(V_{DPPC} - V_{chol} + C)x_c + V_{DPPC}.\end{aligned} \tag{3}$$

Therefore, we can estimate the partial molecular volumes in the phase as

$$V_{DPPC} = \overline{V}^*(0) \tag{4}$$

and

$$V_{chol} = \overline{V}^*(1) + C. \tag{5}$$

2.3. Fluorescence experiment

DPPC and cholesterol were dissolved in methanol and in hexane/2-propanol (3 : 2, v/v), respectively and mixed at an appropriate mole ratio. The fluorescence probe tPA in methanol was added at the DPPC/tPA mole ratio of 200:1 [16]. The obtained solution was dried under nitrogen flow and in vacuum, and the resulting lipid film was dissolved into distilled and deionized water. The final concentration of DPPC was 200 μM. The fluorescence experiments were performed with a FluoTime 200 spectrometer (PicoQuant). The excitation and emission wavelengths were 298 nm and 405 nm, respectively, and the temperature was adjusted to be 45 °C. The fluorescence decay curve $I(t)$ of tPA was analyzed by using a stretched exponential function derived based on a continuous distribution of lifetimes [38–40] as follows:

$$I(t) = \int_{-\infty}^{t} IRF(t) \sum_{i=1}^{n} A_i \exp\left\{-\left(\frac{t-t'}{\tau_i}\right)\right\}^{1/h_i} dt', \tag{6}$$

where $IRF(t)$ and τ_i are the impulse response function and the characteristic time scale of the decay, respectively. When the heterogeneity parameter h_i is 1, the decay is a simple exponential process.

When two stretched exponential functions ($n = 2$) were used to analyze the decay profile in the L_d/L_o coexistence region, the fractional fluorescence intensity of component 1 (domain fraction R_1) was numerically calculated by the following equation:

$$R_1 = \frac{\int_0^\infty A_1 \exp\{-(t/\tau_1)\}^{1/h_1} dt}{\int_0^\infty A_1 \exp\{-(t/\tau_1)\}^{1/h_1} dt + \int_0^\infty A_2 \exp\{-(t/\tau_2)\}^{1/h_2} dt}. \tag{7}$$

3. Results

3.1. Detailed volumetric behavior of DPPC/cholesterol binary bilayers

In order to examine the molecular interaction in DPPC/cholesterol binary bilayers, we scrutinized the dependence of their specific volume on cholesterol mole fraction x_c at constant temperature by the neutral flotation method (Fig. 2). We measured the specific volume of the binary bilayer $\overline{v}(x_c)$ with more cholesterol concentrations (the x_c interval of about 0.03) than in previous studies to quantitatively analyze the molecular volume behavior (Fig. 2A and B), and calculated the molecular volume deviating from an appropriate straight line $\overline{V}^*(x_c)$ as described in Materials and methods (Fig. 2C and D). Although in principle, we had better use the molecular volume for the analysis of the phase behavior rather than the specific volume of the bilayer, the latter can be helpful especially in the assignment of the phase boundary. We divided the obtained specific volume profiles into three regions based on the break points and the linearity.

At temperatures above the main transition temperature of the pure DPPC bilayer ($T_m = 41.5$ °C [1–3]), regions I ($x_c < x_1$) and III ($x_c > x_2$) are the regions where $\overline{V}^*(x_c)$ showed linearity at the lower and higher x_c ends, respectively (Fig. 2) and region II is in between ($x_1 < x_c < x_2$). These three regions correspond to the L_d phase, the L_d to L_o transition region and the L_o phase, respectively [26,32–35]. The volumetric behaviors shared the fundamental characteristics, irrespective of the temperature; (1) $\overline{v}(x_c)$ in the region I (the L_d phase) decreased with increasing x_c, (2) $\overline{v}(x_c)$ in the region III (L_o phase) increased with increasing x_c and (3) $\overline{V}^*(x_c)$ in the region II was located below the straight line connecting the data points at x_1 and x_2, indicating the volumetric behavior in the

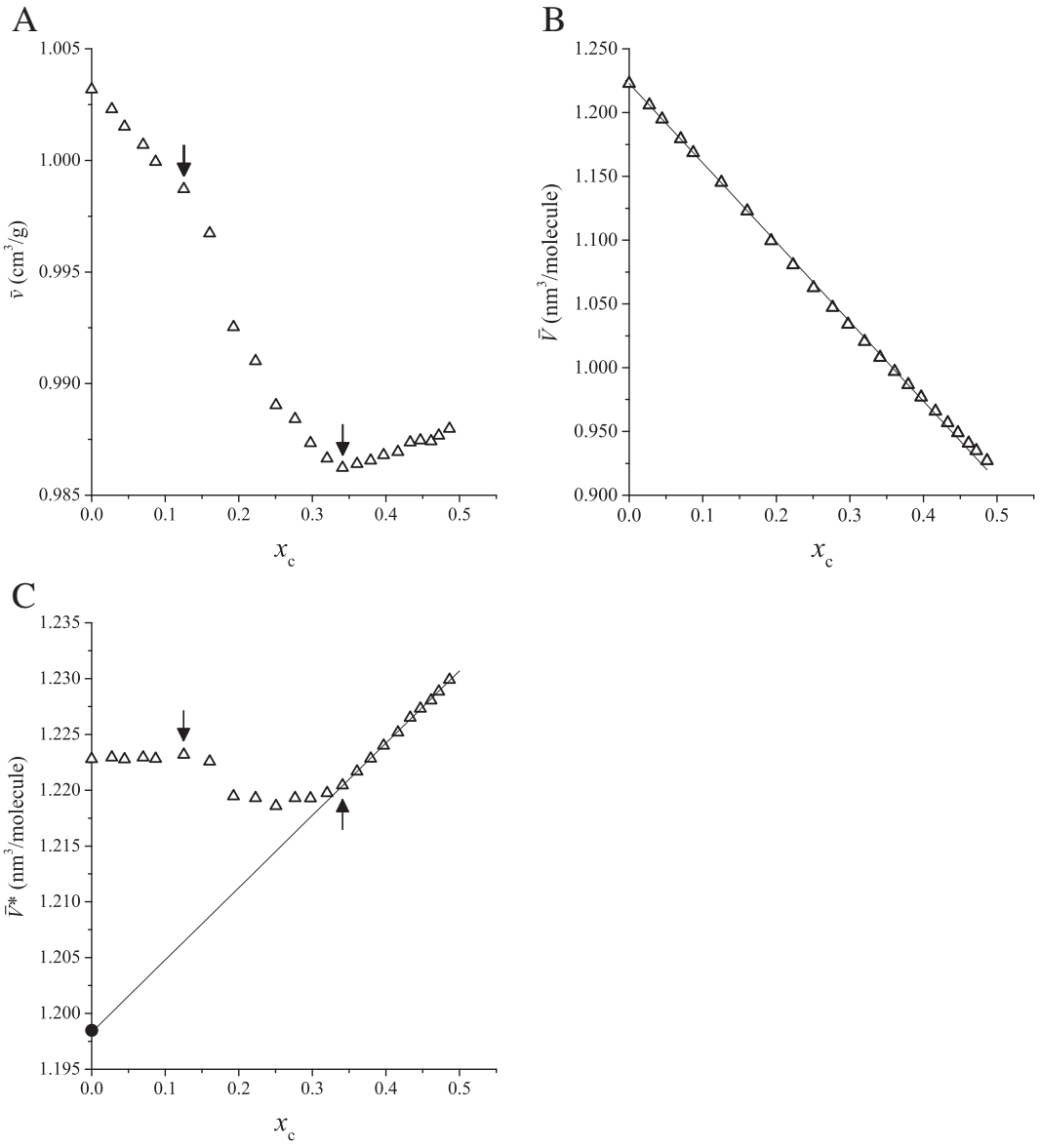

Fig. 1. Analysis procedure for buoyant density measurements. (A) Dependence of the specific volume of DPPC/cholesterol binary bilayers $\bar{v}$ on cholesterol mole fraction x_c. Temperature was kept at 45 ± 0.5 °C. Breakpoints corresponding to the boundaries between the regions I, II and III (see text for details) are indicated by arrows. (B) The average specific volume per molecule $\bar{v}(x_c)$ and (C) $\bar{v}*(x_c) = \bar{V}(x_c) - Cx_c$ were calculated, where C is the gradient of $\bar{v}(x_c)$ in the low x_c region (indicated by a straight line in (B)), so as to make the deviation from linearity clear. The partial molecular volume of DPPC in the region III was estimated by fitting the $\bar{v}*(x_c)$ data to a straight line and extrapolating the line to $x_c = 0$ (closed circle in (C)).

region II cannot be explained by simple coexistence of the L_d and L_o domains (see Discussion for details).

The x_1 value was about 0.15, depending little on temperature in the range we examined (45–55 °C) though the variation of $\bar{V}^*(x_c)$ in the vicinity of x_1 seemed to become less discrete and more ambiguous as the temperature increased. On the other hand, the x_2 value was shifted toward higher x_c with increasing temperature.

Below T_m, we selected the temperatures below the pretransition temperature of the pure DPPC bilayer (~35 °C [2,3]) for measurements of $\bar{v}(x_c)$ as the volumetric behavior was expected to be somewhat complicated near T_m because of the existence of the ripple phase. The $\bar{v}(x_c)$ increased with increasing x_c in contrast to the effect of cholesterol at temperatures above T_m, whereas there appeared to be linear regions at the lower and higher x_c ends in the temperature range of 25–35 °C as at temperatures above T_m (Fig. 2B and D). Therefore, the specific volume profiles can be divided into three regions IV, V and VI as previously described using different methods [36,37,41], although it was difficult to accurately determine the boundary because of the small variation in the gradient at the breakpoints x_3 and x_4. The regions IV, V and VI correspond to the gel phase, the gel to L_o transition region and the L_o phase, respectively. The x_3 value was estimated to be about 0.05 below 30 °C and about 0.1 at 35 °C. In the region IV at 35 °C, the linearity of $\bar{v}(x_c)$ was somewhat ambiguous and its gradient seemed to change gradually probably because the temperature is near the pretransition temperature and the ripple phase may coexist with the gel phase. The x_4 value seemed to shift gradually toward higher x_c as the temperature decreased, although the number of data points belonging to the region VI at 25 °C was too few to be unequivocally conclusive. As for the region V, the deviation from linearity was small except for the profile at 30 °C, which seemed to cross a phase boundary possibly between the gel /L_o and ripple /L_o coexistence regions at x_c ~ 0.3.

Based on the results described above, we made a rough phase diagram for the DPPC/cholesterol binary bilayer system (Fig. 3).

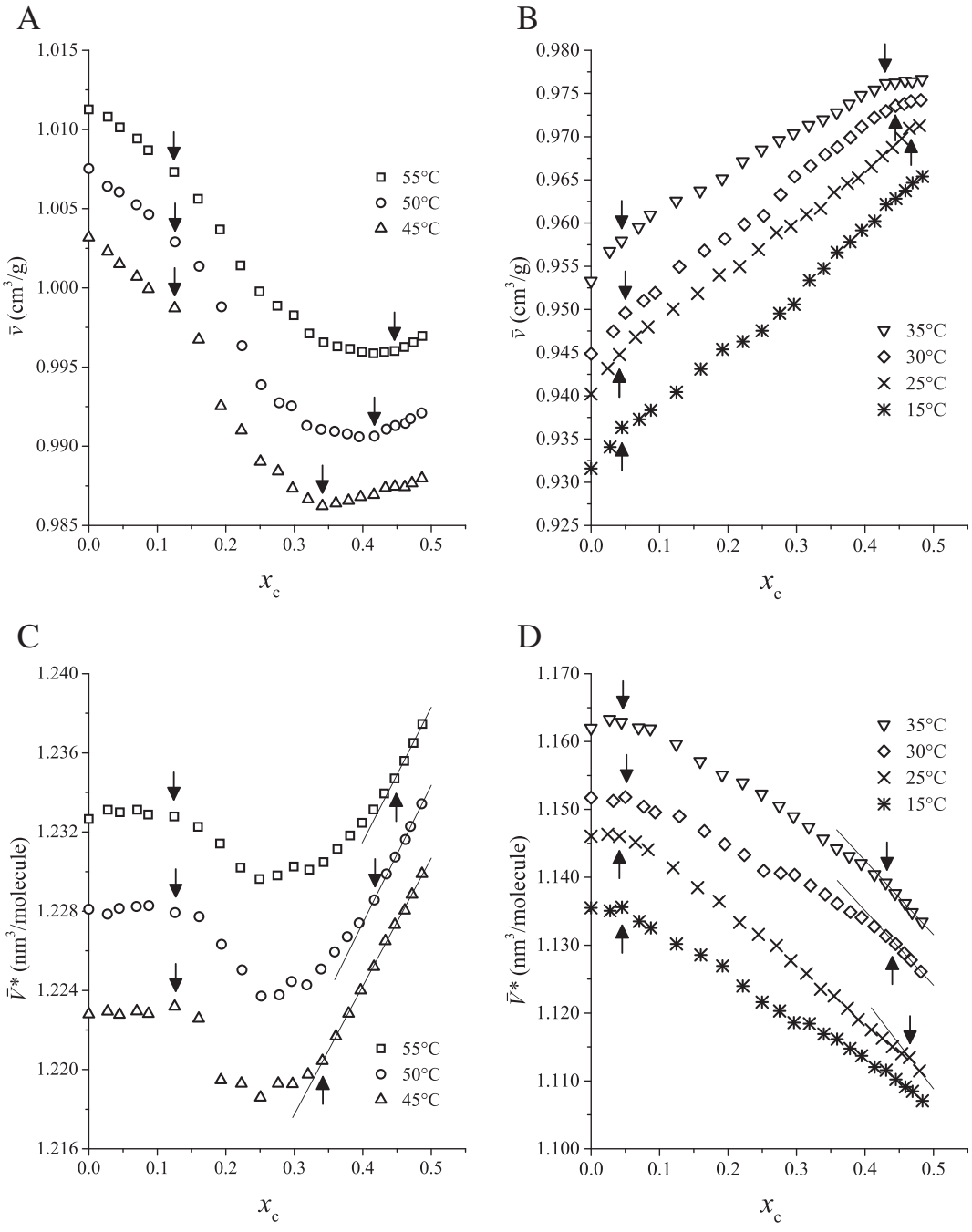

Fig. 2. Dependence of the specific volume of the DPPC/cholesterol binary bilayer $\bar{v}(x_c)$ on cholesterol mole fraction x_c at the temperatures (A) above the main transition and (B) below the pretransition. The $\bar{v}*(x_c)$ profiles corresponding to (A) and (B) are shown in (C) and (D), respectively. The straight lines fitted to the data in the high-x_c region are to make clear the deviation from linearity. Breakpoints corresponding to phase boundaries are indicated by arrows (see text for details). The profile at 45 °C seems to have discontinuity at $x_c \sim 0.15$. However, this may be caused by inaccuracy of the measurement because of the fairly sharp gradient in this x_c range. Raw data will be supplied to interested readers upon request.

3.2. Estimation of partial molecular volumes of DPPC and cholesterol

The partial molecular volumes of DPPC (V_{DPPC}) and cholesterol (V_{chol}) in the regions I (the L_d phase), IV (the gel phase), III and VI (the L_o phase) were estimated (Fig. 4). The partial molecular volumes were almost linearly dependent on temperature with roughly the same gradient, irrespective of the molecular species and the phase. The partial molecular volume of DPPC in the regions III and VI seem to depend linearly on temperature from 25 °C to 55 °C and lie just in the middle between those in the L_d phase (V^{Ld}_{DPPC}) and the gel phase (V^{gel}_{DPPC}), which is consistent with the continuity of these regions as a single L_o phase. It should be mentioned that the change of V_{DPPC} in the cholesterol-induced L_d to L_o phase transition was only about 3 %, whereas the change in the partial lipid area induced by cholesterol has been reported to be much larger (> 20 % in the DMPC/cholesterol binary bilayer system) [42]. In contrast to V_{DPPC}, V_{chol} was larger in the order of $V^{gel}_{chol} > V^{Lo}_{chol} > V^{Ld}_{chol}$, and V^{Lo}_{chol} lay nearer to V^{Ld}_{chol} than to V^{gel}_{chol}.

The obtained partial molecular volumes are summarized in Tables 1 and 2 together with the x_c values at the phase boundaries.

3.3. Detection of phase boundaries by using a fluorescent probe tPA

We measured the fluorescence decay of tPA added into DPPC/cholesterol binary bilayers with more cholesterol concentrations. The fluorescence decay profile at 45 °C was fitted to a stretched exponential function as described in the Materials and methods, and

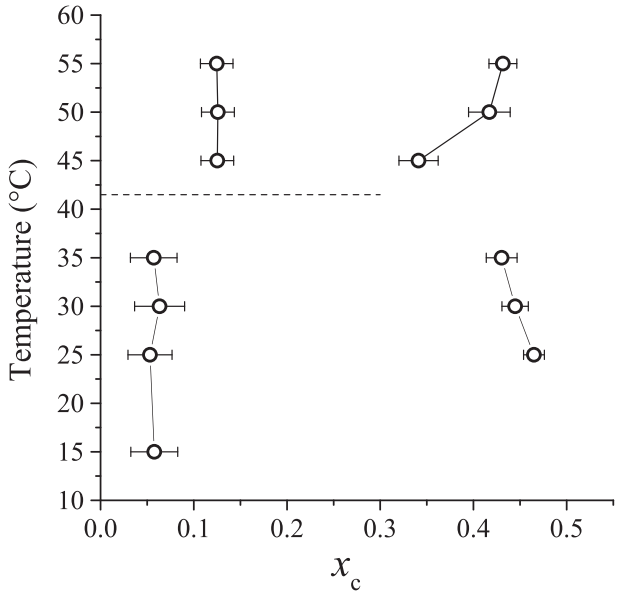

Fig. 3. The phase diagram of the DPPC/cholesterol binary bilayer system constructed on the basis of $\bar{v}(x_c)$ and $\bar{v}*(x_c)$ in Fig. 2. Since it is difficult to definitely determine the phase boundary, the ranges of likely boundaries are indicated by horizontal bars. Particularly the value of x_3 was ambiguous because of small change in gradient of $\bar{v}(x_c)$ at the boundary and existence of the ripple phase.

the dependence of the fitting parameters on x_c is shown in Fig. 5. Both the characteristic time scale τ (Fig. 5A) and the heterogeneity parameter h (Fig. 5B) indicated that their x_c dependences were consistent with that of the specific volume shown in Fig. 2, indicating the existence of the phase boundaries at $x_c \approx 0.12$ and 0.34 (45 °C). The value of τ was nearly constant in the L_d phase ($0 \le x_c \le 0.12$) and the L_o phase ($x_c \ge 0.34$), whereas it increased in the region between L_d and L_o phases ($0.12 \le x_c \le 0.34$) probably because fluorescence decays of tPA molecules in the two phases were superposed (see Discussion for details). The heterogeneity parameter tended to decrease, approaching to 1.0 as x_c increased, suggesting that the distribution of the tPA molecules mobility becomes narrower as the lipid molecular packing becomes more ordered.

4. Discussion

4.1. Partial molecular volume of DPPC and cholesterol

We carefully measured specific volumes of DPPC/cholesterol binary bilayers with more cholesterol concentrations, and consequently obtained the partial molecular volumes of DPPC and cholesterol in the L_d, L_o and gel phases with high accuracy (Fig. 4). We found that the partial molecular volume of DPPC in the L_o phase V_{DPPC}^{Lo} is just in the middle between V_{DPPC}^{Ld} and V_{DPPC}^{gel} and the differences between the values in these three phases were fairly small as the volume change of a DPPC molecule in the cholesterol-induced L_d/L_o phase transition is only a few percent.

The question is what is the origin of the molecular volume difference between the phases. Cevc [43] and Marsh [26] discussed the origin of the specific volume difference of pure phospholipid bilayers between the L_d/L_o and gel phases, and pointed out that the *trans-gauche* chain isomerization is the likely candidate to result in the specific volume difference. More recent detailed analysis of the molecular volumes [4] suggested that contribution of the headgroup volume is negligible and the molecular volume difference between the gel and L_d phases is attributed to the change in the hydrocarbon chain volume: the hydrocarbon chain volume in a DPPC molecule was estimated to be 0.825 nm^3 at 20 °C and 0.913 nm^3 at 50 °C, which almost fully explains the difference $V_{DPPC}^{Ld} - V_{DPPC}^{gel}$ shown in Fig. 4. If it is also the case for in the molecular volume in the L_o phase, then the hydrocarbon chain state in the L_o phase is just intermediate between those in the L_d and gel phases. Although highly speculative, it is interesting to interpret that in the L_o phase one of the DPPC hydrocarbon chains is in the gel state and the other in the L_d state.

Another possibility is the difference in hydration state [44,45]. We analyzed the data assuming that the density of water in the inside of the bilayer vesicle is equal to that of the bulk water. If the density of hydrated water located between bilayers is different from that of bulk water, the density difference is involved in the measured data

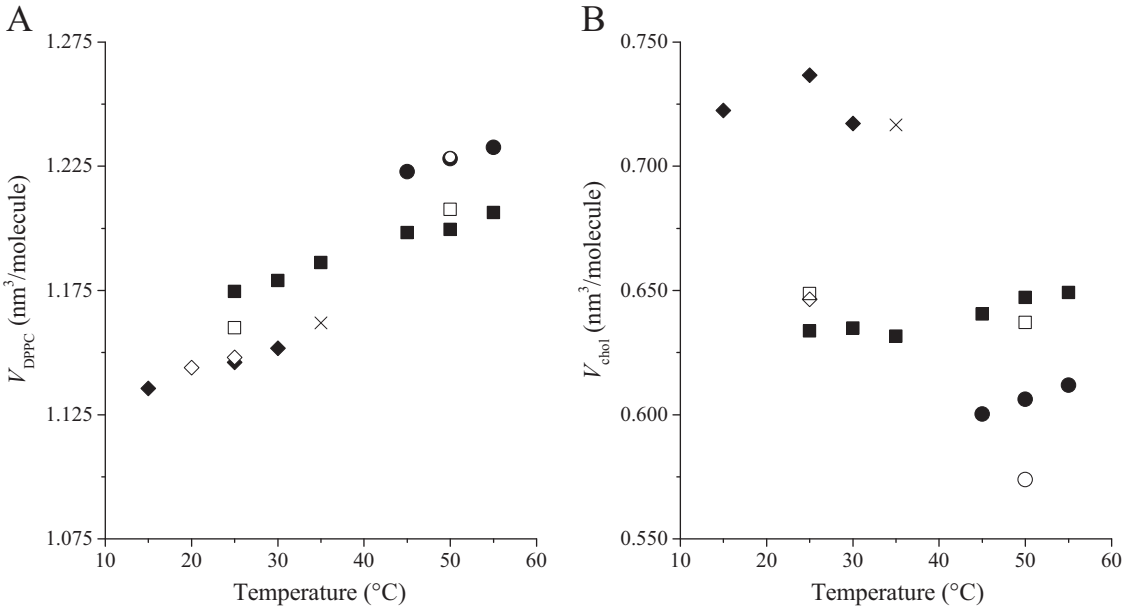

Fig. 4. Temperature dependence of partial molecular volumes of (A) DPPC V_{DPPC} and (B) cholesterol V_{chol} in the L_d phase (●), the L_o phase (■) and the gel phase (◆). As the ripple phase may coexist with the gel phase in the low x_c region at 35 °C, a mark (×) different from that for the gel phase is used. The partial molecular volume of cholesterol may have a larger error than that of DPPC because of extrapolation to a far x_c value. Some older data are also shown for comparison [4,36]; the L_d phase (○), the L_o phase (□) and the gel phase (◇).

Table 1
Summary of the data obtained above T_m.

Temperature (°C)	x_1	x_2	V^{Ld}_{DPPC}(nm^3)	V^{Lo}_{DPPC}(nm^3)	V^{Ld}_{chol}(nm^3)	V^{Lo}_{chol}(nm^3)	Ref
45	0.125	0.341	1.223	1.198	0.600	0.640	
50	0.126	0.417	1.228	1.200	0.606	0.647	
			1.229	1.208	0.574	0.637	[36]
55	0.125	0.432	1.233	1.206	0.612	0.649	

depending on the number of the hydrated water. Even if the density difference is small, it could contribute to the specific volume difference between phases shown in Fig. 4, considering that the difference in the number of hydrated water molecules between the L_d and gel phases is in the order of 10 per molecule [43]. When the density of H_2O/D_2O solvent is balanced with that of the bilayer vesicle, which consists of bilayer membrane and hydrated water, the difference of the bilayer membrane density from the solvent density $\Delta\rho_b$ (> 0) is related to the difference of the hydrated water density from the solvent density $\Delta\rho_w$ (< 0) as $\Delta\rho_b = -(\Delta n V_w/V_b)\Delta\rho_w$, where V_w, V_b and n are the volume of a hydrated water molecule, the average volume of the bilayer membrane and the number of hydrated waters per lipid molecule, respectively. If $V_w = 0.03$ nm^3 (the volume of a bulk water molecule), $V_b = 1$ nm^3 (Fig. 4) and $\Delta\rho_w = -0.03$ g/cm^3 (the density difference estimated by Wiener et al. [45]), $\Delta\rho_b$ is calculated to be $0.0009\,n$ g/cm^3. Therefore, the density difference between the bilayer membranes in the L_d and gel phases resulting from change in the number of hydrated water molecules is estimated to be 0.009 g/cm^3, which can explain only a little part of the molecular volume difference between these two phases shown in Fig. 4A. Therefore, the contribution of hydration to the molecular volume difference between the phases must be small.

In contrast to V_{DPPC}, V_{chol} seemed to change to a greater degree (Fig. 4B). The relative volume difference between the L_d and gel phases $(V^{gel}_{chol} - V^{Ld}_{chol})/V^{Ld}_{chol}$ was about 20%, which is much larger than previously described by Greenwood et al. [36]; using data obtained by Melchior et al. [37] they estimated both V^{gel}_{chol} and V^{Lo}_{chol} to be about 0.65 nm^3 at 25 °C. We estimated the V^{Lo}_{chol} to be about 0.63 nm^3, which agrees well with their value whereas the V^{gel}_{chol} is larger by ~0.1 nm^3 (Fig. 4B and Table 1). This disagreement may be caused by inaccurate estimation of V^{Lo}_{chol} due to the insufficient number of data points and the low trustworthiness of far extrapolation. We think that our data are more reliable because the V^{gel}_{chol} values at different temperatures fall in a narrow range (Fig. 4B).

The partial molecular volume in the L_d phase V^{Ld}_{chol} was estimated to be about 0.6 nm^3, which is a little less than the molecular volume (0.628 nm^3) in an anhydrous cholesterol crystal calculated from the lattice parameters [46,47]. Therefore, it is likely that sparsely distributed cholesterol molecules are surrounded closely by DPPC molecules in the fluid state without an interaction volume (interstitial void volume). On the other hand, mismatch in shape between neighboring DPPC and cholesterol molecules may bring forth a fairly large interaction volume in the gel phase.

Since the interaction volume comes from the interaction between neighboring molecules, we should take into account how it is divided between V_{DPPC} and V_{chol} as explained by Greenwood et al. [36]. This problem was quantitatively discussed by Edholm and Nagle [18] for analyzing simulation data. Here, we used a simpler model to understand the extent of incorporation of the interaction volume in V_{DPPC} and V_{chol} (Appendix A). Simple calculation reveals that in the L_d and gel phases, where x_c is small, the interaction volume is incorporated mostly into V_{chol} and little into V_{DPPC}. Therefore, it is likely that in the gel to L_d transition the change in V_{chol} ($\Delta V_{chol} \sim -0.13$ nm^3) is larger than that in V_{DPPC} ($\Delta V_{DPPC} \sim +0.08$ nm^3) due to fairly large interaction volume formed in the gel phase.

We have probably underestimated the effect of the interaction volume on the partial molecular volume in the L_o phase (see Appendix A). If the difference between cholesterol molecules in the L_d and L_o phases is mostly attributed to the interaction volume and the calculation described in Appendix A is a good estimate, the actual size of the interaction volume is significantly larger than the difference $V^{Lo}_{chol} - V^{Ld}_{chol}$ obtained from Fig. 4B. Thus, the molecular state of cholesterol in the L_o phase may be closer to that in the gel phase than expected from Fig. 4B.

McMullen et al. [48,49] proposed that hydrophobic mismatch between phospholipid and cholesterol molecules, which is the smallest for diheptadecanoylphosphatidylcholine, causes the difference in the transition behavior. Since the hydrophobic mismatch is closely related to the interaction volume, it is interesting to investigate the effect of the phospholipid hydrocarbon chain length on the partial molecular volumes.

4.2. The L_d to L_o transition region

We made a rough phase diagram of the DPPC/cholesterol binary bilayer system based on our volumetric measurements (Fig. 3). The obtained phase diagram shares basic features with those previously summarized by Marsh [26]. The phase boundary at x_4 in Fig. 3 is evidently located at a higher value of x_c than that seen in other phase diagrams. However, the positions of phase boundaries differ greatly from diagram to diagram [26,32–35] and are mutually inconsistent. Hence, we focus below on the features of the intermediate L_d to L_o transition region (region II) rather than the phase diagram itself as we found a new volumetric behavior in this region.

Fig. 2C shows that the values of $\overline{V}(x_c)$ in the region II deviated from linearity. Assuming that the L_d and L_o phases coexist without mutual interaction in the region II and the ratio of their domains is kept constant irrespective of x_c, $\overline{V}(x_c)$ must be linear in the region II. According to the lever rule, proportions of coexisting L_d and L_o phases at the given temperature are determined as $(x_2 - x_c) : (x_c - x_1)$ [50] and the composition ratios (DPPC/cholesterol) in these two phases are fixed at the values at x_1 and x_2, respectively. Therefore, the deviation from the lever rule means that the composition ratio depends on x_c. If we can neglect the condition of the constant composition ratio, we can make

Table 2
Summary of the data obtained below T_m.

Temperature (°C)	x_3	x_4	V^{gel}_{DPPC}(nm^3)	V^{Lo}_{DPPC}(nm^3)	V^{gel}_{chol}(nm^3)	V^{Lo}_{chol}(nm^3)	Ref
15	0.058	–	1.136	–	0.723	–	
25	0.053	0.465	1.146	1.175	0.737	0.634	
			1.148	1.160	0.647	0.649	[36]
30	0.063	0.445	1.152	1.176	0.717	0.638	
35	0.057	0.430	1.162	1.181	0.711	0.637	

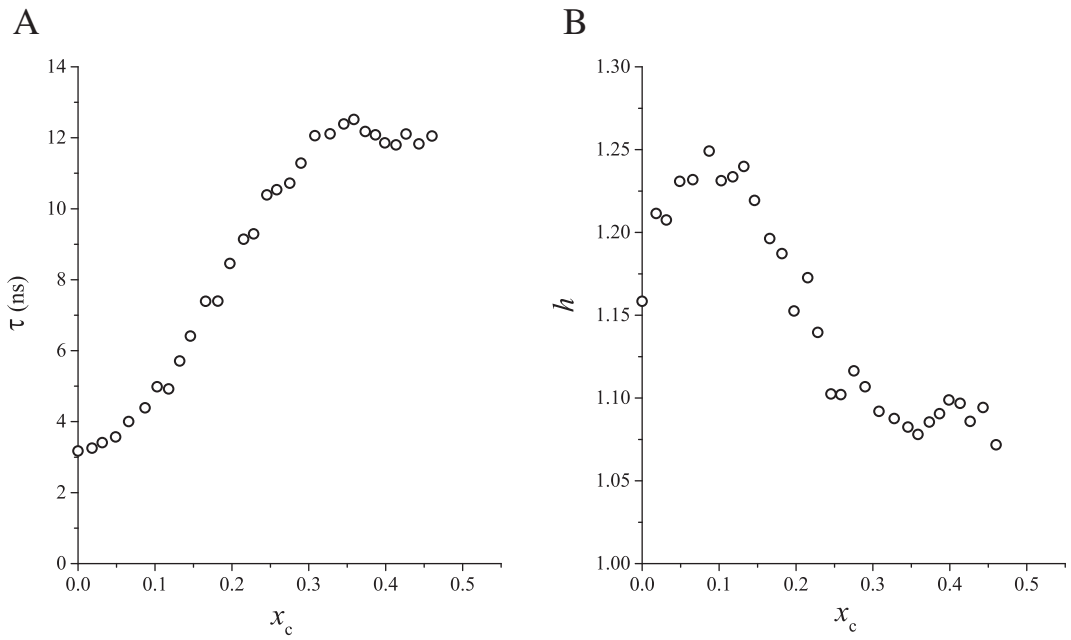

Fig. 5. Analysis of the fluorescence decay of tPA added to DPPC/cholesterol binary bilayers at 45°C. We fitted the decay curve to a stretched exponential function including a characteristic time scale τ and a heterogeneity parameter h (see Materials and methods). Dependence of (A) τ and (B) h on x_c is shown.

a model to explain the deviation: For example, simple simulation can fit the nonlinear data, assuming that cholesterol molecules are randomly distributed and the L_o phase forms in the region with an appropriate size, where the local cholesterol mole ratio becomes higher than a threshold mole ratio (data not shown). In this simulation, the composition ratio of DPPC and cholesterol molecules in each of the two coexisting domains changes depending on x_c. This implies that these states must be nonequilibrium, considering that in equilibrium the chemical potential of DPPC/cholesterol, which depends on the composition ratio, is kept constant irrespective of x_c. We infer that the system is in an equilibrium state and the lever rule is applicable in the L_d/L_o coexistence region as the molecules are likely to be highly mobile in these phases.

To obtain experimental evidence for the lever rule, we tried to analyze the fluorescence decay profile in the L_d/L_o coexistence region using two characteristic time scales (Fig. 6A). As a result, the fitting with two stretched exponential functions was converged properly only at $0.1 < x_c < 0.3$ with keeping the two characteristic time scales almost constant ($\tau_1 \sim 4$ ns, $\tau_2 \sim 12$ ns), suggesting the existence of two definitely separated phases (Fig. 6A). Moreover, the domain fraction

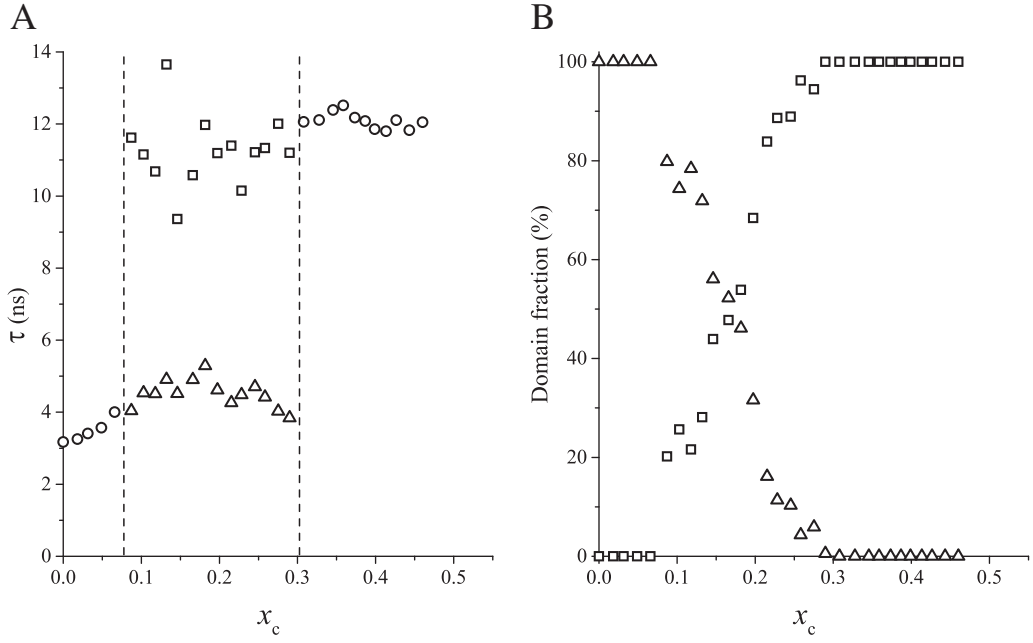

Fig. 6. Analysis of the fluorescence decay of tPA using two stretched exponential functions. Curve fitting was properly converged only in the range of $x_c = 0.1 \sim 0.3$, where two characteristic time scales were kept roughly constant irrespective of x_c (A). We estimated the domain fraction of the L_d phase (△) and the L_o phase (□) in their coexistence region as a ratio of the integrated intensities of the two stretched functions (B).

R_1 seemed to follow the lever rule (Fig. 6B). However, these fittings were little better than those obtained using a stretched exponential and the coexistence region in Fig. 6B is slightly shifted toward lower x_c, in comparison with that expected from Fig. 4 B. It is unlikely that this shift is caused by the addition of the fluorescent probe tPA because it was reported to have little effect on the phase diagram of the DMPC/cholesterol binary bilayers [51]. Thus, further study is needed to confirm that the lever rule is applicable under these circumstances.

Finally, we would like to point out one more possibility that there exists an intermediate phase between the L_d and L_o phases. It seemed that the average molecular volume profile $\overline{V}(x_c)$ may not be smooth in the L_d/L_o coexistence region and have a turning point (see the region of $0.25 < x_c < 0.35$ in Fig. 4B, which seemed to be on a straight line). If it is the case, the coexistence region should be divided into two regions, i.e., L_d/ intermediate and intermediate /L_o regions of phase coexistence.

It is not possible to conclude what is reasonable for the origin of the deviation from linearity in $\overline{V}(x_c)$ in the coexistence region. Further systematic study such as investigation on chain length dependence of $\overline{V}(x_c)$ and study using other methods with more cholesterol concentrations are required to obtain a deeper insight into the domain structure.

5. Conclusion

We examined cholesterol-induced formation of the L_o phase in DPPC/cholesterol binary bilayers by measuring their specific volume using density-controlled H_2O/D_2O solvents and analyzing the fluorescence decay profile of a fluorescent probe (*trans*-parinaric acid). Measurements with many cholesterol concentrations and careful experimental procedure made it possible to obtain the detailed volumetric behaviors, especially at temperatures higher than the main transition, and to provide reliable basic data for discussion about phospholipid–cholesterol interaction in the L_o phase. Based on the obtained data, we drew a rough phase diagram. We found that the average molecular volume in the L_d/L_o coexistence region deviates from linearity, indicating inapplicability of simple additivity of the volumes of two phase domains. Moreover, on the basis of linear dependence of the average molecular volume of the cholesterol mole fraction, we estimated partial molecular volumes of DPPC and cholesterol in the L_d, L_o and gel phases. The partial molecular volumes obtained in the L_o phase suggest that the hydrocarbon chain state in the L_o phase is intermediate between those of the gel and L_d phases.

Acknowledgments

We would like to thank Dr. Naoto Tamai (Kwansei Gakuin University) for his useful discussion about the fluorescence experiment. This work was partially supported by the MEXT-Supported Program for the Strategic Research Foundation at Private Universities (S1201027) 2012–2016.

Appendix A. Effect of the interaction volume on the partial molecular volume

The extra volume (interaction volume) resulting from intermolecular interaction should be incorporated into the average molecular volume as a function depending on the number of relevant molecular pairs. Assuming for simplicity that cholesterol–DPPC interaction is the major supplier of the interaction volume and one cholesterol molecule randomly distributed in a bilayer is surrounded by 6 hydrocarbon chains (cholesterol is counted as a hydrocarbon chain), the volume of the bilayer containing N molecules is calculated as:

$$N\overline{V} = N_C V_C + N_D V_D + \frac{2N_D N_C}{2N_D + N_C} V_v, \tag{A1}$$

where N_C, N_D, V_C and V_D are the number and the volume of cholesterol and DPPC molecules, respectively, and V_v is the sixfold of the interaction volume resulting from a cholesterol–DPPC hydrocarbon chain pair, the number of which is $12N_DN_C/(2N_D + N_C)$. Therefore, the average specific volume per molecule $\overline{V}$ can be written as a function of cholesterol mole fraction $x_c = N_C/N$.

$$\overline{V}(x_c) = x_c V_C + (1-x_c)V_D + \frac{2x_c^2 - 8x_c + 4}{(2-x_c)^2} V_v. \tag{A2}$$

Since V_v is usually small, the nonlinearity resulting from the third term is not prominent. Therefore, in this study, we estimated the partial molecular volumes of DPPC and cholesterol by linear approximation. Roughly speaking, the straight line to which we fitted the data may be approximated to the tangent of $\overline{V}(x_c)$ at the center of the x_c range used for analysis x_a:

$$\overline{V}(x_c) = \left\{ V_C - V_D + \frac{2x_a^2 - 8x_a + 4}{(2-x_a)^2} V_v \right\} x_c + V_D + \frac{2x_a^2}{(2-x_a)^2} V_v. \tag{A3}$$

If this is a good approximation, the interaction volume is incorporated into the partial molecular volume we estimated as follows:

$$V_{DPPC} = \overline{V}(0) = V_D + \frac{2x_a^2}{(2-x_a)^2} V_v \tag{A4}$$

and

$$V_{chol} = \overline{V}(1) = V_C + \frac{4(1-x_c)^2}{(2-x_a)^2} V_v. \tag{A5}$$

These equations imply that the interaction volume is included mostly in V_{chol} and little in V_{DPPC} in the L_d and gel phases because $x_a \ll 1$ in the analysis of these phases. On the other hand, the contribution of V_v to V_{DPPC}^{Lo} and V_{chol}^{Lo} is estimated to be about 13% and 56%, respectively, as $x_a \approx 0.4$ in the analysis of the L_o phase. Although the assumption of 6 hydrocarbon chains surrounding one cholesterol molecule is an oversimplified assumption, it must be true that the effect of interaction volume on the partial molecular volumes in the L_o phase is underestimated.

References

[1] S. Ohtake, C. Schebor, J.J. Pablo, Effects of trehalose on the phase behavior of DPPC–cholesterol unilamellar vesicles, Biochim. Biophys. Acta 1578 (2006) 65–73.
[2] D.A. Mannock, R.N.A.H. Lewis, R.N. McElhaney, Comparative calorimetric and spectroscopic studies of the effects of lanosterol and cholesterol on the thermotropic phase behavior and organization of dipalmitoylphosphatidylcholine bilayer membranes, Biophys. J. 91 (2006) 3327–3340.
[3] D.A. Mannock, R.N.A.H. Lewis, R.N. McElhaney, A calorimetric and spectroscopic comparison of the effects of ergosterol and cholesterol on the thermotropic phase behavior and organization of dipalmitoylphosphatidylcholine bilayer membranes, Biochim. Biophys. Acta 1798 (2010) 376–388.
[4] J.F. Nagle, S.T. Nagle, Structure of lipid bilayers, Biochim. Biophys. Acta 1469 (2000) 159–195.
[5] S. Karmakar, V.A. Raghunathan, Structure of phospholipid–cholesterol membranes: an X-ray diffraction study, Phys. Rev. E. 71 (2005) 061924.
[6] T.T. Mills, G.E.S. Toombes, S.T. Nagle, D.M. Smilgies, G.W. Feigenson, J.F. Nagle, Order parameters and areas in fluid-phase oriented lipid membranes using wide angle X-ray scattering, Biophys. J. 95 (2008) 669–681.
[7] T.T. Mills, S.T. Nagle, F.A. Heberle, N.F. Morales, J. Zhao, J. Wu, G.E.S. Toombes, J.F. Nagle, G.W. Feigenson, Liquid–liquid domains in bilayers detected by wide angle X-ray scattering, Biophys. J. 95 (2008) 682–690.
[8] A. Ivankin, I. Kuzmenko, D. Gidalevitz, Cholesterol–phospholipid interactions: new insights from surface X-ray scattering data, Phys. Rev. Lett. 104 (2010) 108101.
[9] M.R. Vist, J.H. Davis, Phase equilibria cholesterol/dipalmitoylphosphatidylcholine mixtures: 2H nuclear magnetic resonance and differential scanning calorimetry, Biochemistry 29 (1990) 451–464.
[10] H. Reinl, T. Brumm, T.M. Bayerl, Changes of the physical properties of the liquid-ordered phase with temperature in binary mixtures of DPPC with cholesterol: a ^{2}H-NMR, FT-IR, DSC, and neutron scattering study, Biophys. J. 61 (1992) 1025–1035.
[11] B.B. Bonev, M.R. Morrow, ^{2}H NMR studies of dipalmitoylphosphatidylcholine and dipalmitoylphosphatidylcholine-cholesterol bilayers at high pressure, Can. J. Chem. 76 (1998) 1512–1519.

[12] J.A. Clarke, A.J. Heron, J.M. Seddon, R.V. Law, The diversity of the liquid ordered (L_o) phase of phosphatidylcholine/cholesterol membranes: a variable temperature multinuclear solid-state NMR and x-ray diffraction study, Biophys. J. 90 (2006) 2383–2393.
[13] J. Zhao, J. Wu, F.A. Heberle, T.T. Mills, P. Klawitter, G. Huang, G. Costanza, G.W. Feigenson, Phase studies of model biomembranes: complex behavior of DSPC/DOPC/cholesterol, Biochim. Biophys. Acta 1768 (2007) 2764–2776.
[14] B.M. Castro, L.C. Silva, A. Fedorov, R.F.M. de Almeida, M. Prieto, Cholesterol-rich fluid membranes solubilize ceramide domains: implications for the structure and dynamics of mammalian intracellular and plasma membranes, J. Biol. Chem. 34 (2009) 22978–22987.
[15] T. Baumgart, G. Hunt, E.R. Farkas, W.W. Webb, G.W. Feigenson, Fluorescence probe partitioning between L_o/L_d phases in lipid membranes, Biochim. Biophys. Acta 1768 (2010) 2182–2194.
[16] T.K.M. Nyholm, D. Lindroos, B. Westerlund, J.P. Slotte, Construction of a DOPC/PSM/cholesterol phase diagram based on the fluorescence properties of *trans*-parinaric acid, Langmuir 27 (2011) 8339–8350.
[17] H.I. Petrache, S.E. Feller, J.F. Nagle, Determination of component volumes of lipid bilayers from simulations, Biophys. J. 70 (1997) 2237–2242.
[18] O. Edholm, J.F. Nagle, Areas of molecules in membranes consisting of mixtures, Biophys. J. 89 (2005) 1827–1832.
[19] P.F. Almeida, A simple thermodynamic model of the liquid-ordered state and the interactions between phospholipids and cholesterol, Biophys. J. 100 (2011) 420–429.
[20] S.L. Duncan, I.S. Dalal, R.G. Larson, Molecular dynamics simulation of phase transitions in model lung surfactant monolayers, Biochim. Biophys. Acta 1808 (2011) 2450–2465.
[21] J. Joannis, P.S. Coppock, F. Yin, Makoto Mori, A. Zamorano, J.T. Kindt, Atomistic simulation of cholesterol effects on miscibility of saturated and unsaturated phospholipids: implications for liquid-ordered/liquid-disordered phase coexistence, J. Am. Chem. Soc. 113 (2011) 3625–3634.
[22] K. Simons, E. Ikonen, Functional rafts in cell membranes, Nature 387 (1997) 569–572.
[23] K. Simons, W.L.C. Vaz, Model systems, lipid rafts, and cell membranes, Biophys. Biomol. Struct. 33 (2004) 269–295.
[24] D. Lingwood, K. Simons, Lipid rafts as a membrane-organizing principle, Science 518 (327) (2010) 46–50.
[25] S.L. Veatch, S.L. Keller, Separation of liquid phases in giant vesicles of ternary mixtures of phospholipids and cholesterol, Biophys. J. 85 (2003) 3074–3083.
[26] D. Marsh, Liquid-ordered phases induced by cholesterol: a compendium of binary phase diagrams, Biochim. Biophys. Acta 1798 (2010) 688–699.
[27] A. Radhakrishnan, Phase separations in binary and ternary cholesterol–phospholipid mixtures, Biophys. J. 98 (2010) L41–L43.
[28] J.M. Crane, L.K. Tamm, Role of cholesterol in the formation and nature of lipid rafts in planar and spherical model membranes, Biophys. J. 86 (2004) 2965–2979.
[29] P. Pathak, E. London, Measurement of lipid nanodomain (raft) formation and size in sphingomyelin/POPC/cholesterol vesicles shows TX-100 and transmembrane helices increase domain size by coalescing preexisting nanodomains but do not induce domain formation, Biophys. J. 101 (2011) 2427-2425.
[30] J.R. Silvius, Role of cholesterol in lipid raft formation: lessons from lipid model systems, Biochim. Biophys. Acta 1610 (2003) 174–183.
[31] T.P.W. McMullen, R.N.A.H. Lewis, R.N. McElhaney, Cholesterol–phospholipid interactions, the liquid-ordered phase and lipid rafts in model and biological membranes, Curr. Opin. Colloid Interface Sci. 8 (2004) 459–468.
[32] J.L. Thewalt, M. Bloom, Phosphatidylcholine: cholesterol phase diagrams, Biophys. J. 63 (1992) 1176–1181.
[33] Y.W. Hsueh, K. Gilbert, C. Trandum, M. Zuckermann, J. Thewalt, The effect of ergosterol on dipalmitoylphosphatidylcholine bilayers: a deuterium NMR and calorimetric study, Biophys. J. 88 (2005) 1799–1808.
[34] R. Wu, L. Chen, Z. Yu, P.J. Quinn, Phase diagram of stigmasterol-dipalmitoylphosphatidylcholine mixtures dispersed in excess water, Biochim. Biophys. Acta 1758 (2006) 764–771.
[35] D. Marsh, Cholesterol-induced fluid membrane domains: a compendium of lipid-raft ternary phase diagrams, Biochim. Biophys. Acta 1788 (2009) 2114–2123.
[36] A.I. Greenwood, S.T. Nagle, J.F. Nagle, Partial molecular volumes of lipids and cholesterol, Chem. Phys. Lipids 143 (2006) 1–10.
[37] D.L. Melchior, F.J. Scavitto, J.M. Steim, Dilatometry of dipalmitoyllecithin–cholesterol bilayers, Biochemistry 19 (1980) 4828–4834.
[38] K.C.B. Lee, J. Siegel, S.E. D. Webb, S.L. Fort, M.J. Cole, R. Jones, K. Dowling, M.J. Lever, P.M.W. French, Application of the stretched exponential function to fluorescence lifetime imaging, Biophys. J. 88 (2005) 1799–1808.
[39] I.S. Nikolaev, P. Lodahl, W.L. Vos, Fluorescence lifetime of emitters with broad homogeneous linewidths modified in opal photonic crystals, J. Phys. Chem. C 112 (2008) 7250–7254.
[40] B.R. Fisher, H.J. Eisler, N.E. Stott, M.G. Bawendi, Emission intensity dependence and single-exponential behavior in single colloidal quantum dot fluorescence lifetimes, J. Phys. Chem. B 108 (2004) 143–148.
[41] M.R. Vist, J.H. Davis, Phase equilibria of cholesterol/dipalmitoyl-phosphatidylcholine mixtures: 2H nuclear magnetic resonance and differential scanning calorimetry, Biochemistry 29 (1990) 451–464.
[42] J. Pan, S.T. Nagle, J.F. Nagle, Effect of cholesterol on structural and mechanical properties of membranes depends on lipid chain saturation, Phys. Rev. Lett. 80 (2009).
[43] G. Cevc, Phospholipids Handbook, Marcel Dekker, 1993. 560–561.
[44] M.J. Ruocco, G.G. Shipley, Characterization of the sub-transition of hydrated dipalmitoylphosphatidylcholine bilayers. Kinetic, hydration and structural study, Biochim. Biophys. Acta 691 (1982) 309–320.
[45] M.C. Wiener, S.T. Nagle, D.A. Wilkinson, L.E. Campbell, J.F. Nagle, Specific volumes of lipids in fully hydrated bilayer dispersion, Biochim. Biophys. Acta 938 (1988) 135–142.
[46] B.M. Craven, Pseudosymmetry in cholesterol monohydrate, Acta Crystallogr. B35 (1979) 1123–1128.
[47] D. Bach, E. Wachtel, Phospholipid/cholesterol model membranes: formation of cholesterol crystallites, Biochim. Biophys. Acta 1610 (2003) 187–197.
[48] T.P.W. McMullen, R.N.A.H. Lewis, R.N. McElhaney, Differential scanning calorimetric study of the effect of cholesterol on the thermotropic phase behavior of a homologous series of linear saturated phosphatidylcholines, Biochemistry 32 (1993) 516–522.
[49] T.P.W. McMullen, R.N. McElhaney, New aspects of the interaction of cholesterol with dipalmitoylphosphatidylcholine bilayers as revealed by high-sensitivity differential scanning calorimetry, Biochim. Biophys. Acta 1234 (1995) 90–98.
[50] H.B. Callen, Thermodynamics and an Introduction to the Thermostatics, 2nd ed. John Wiley & Sons, 1985. 239–244.
[51] C.R. Mateo, P. Tauc, J.C. Brochon, Pressure effects on the physical properties of lipid bilayers detected by *trans*-parinaric acid fluorescence decay, Biophys. J. 65 (1993) 2248–2260.